International Journal of Thermal Sciences 106 (2016) 102–111

Contents lists available at ScienceDirect

International Journal of Thermal Sciences

journal homepage: www.elsevier.com/locate/ijts

Analysis of bubble growth on a hot plate during decompression in microgravity

M. Kostoglou [a], T.D. Karapantsios [a, *], C. Colin [b], O. Kannengieser [b]

[a] Division of Chemical Technology, Department of Chemistry, Aristotle University, University Box 116, 541 24 Thessaloniki, Greece
[b] Institut de Mécanique des Fluides de Toulouse, UMR 5502 CNRS-INP-UPS 2, Allée Camille Soula, 31 400 Toulouse, France

ARTICLE INFO

Article history:
Received 12 June 2015
Received in revised form
21 January 2016
Accepted 21 March 2016
Available online 1 April 2016

Keywords:
Decompression
Bubble growth
Mathematical modeling
Analytical solution
Microgravity
Inverse problem

ABSTRACT

The focus of the present work is the modeling of bubble growth on a hot plate during decompression (depressurization) of a volatile liquid at temperatures close to saturation and in the presence of dissolved gas. In particular, this work presents an organized attempt to analyze data obtained from an experiment under microgravity conditions. In this respect, a bubble growth mathematical model is developed and solved at three stages, all realistic under certain conditions but of increasing physical and mathematical complexity: At the first stage, the temperature variation both in time and space is ignored leading to a new semi-analytical solution for the bubble growth problem. At the second stage, the assumption of spatial uniformity of temperature is relaxed and instead a steady linear temperature profile is assumed in the liquid surrounding the bubble from base to apex. The semi-analytical solution is extended to account for the two-dimensionality of the problem. As the predictions of the above models are not in agreement with the experimental data, at the third stage an inverse heat transfer problem is set up. The third stage model considers an arbitrary average bubble temperature time profile and it is solved numerically using a specifically designed numerical technique. The unknown bubble temperature temporal profile is estimated by matching theoretical and experimental bubble growth curves. A discussion follows on the physical mechanisms that may explain the evolution of the average bubble temperature in time.

1. Introduction

Bubble formation, growth and detachment in liquids including dissolved gases when the ambient pressure decreases is a very important process in diverse scientific fields, e.g. in cavitating turbines and pumps [1]; in carbonated drinks [2], in liquid waste treatment by dissolved air flotation [3]. In the past, *liquid degassing* focused mainly on the mechanisms of nucleation rather than bubble dynamics, e.g. see [4]. Therefore, tests were conducted at low temperatures where the role of liquid vapor pressure is negligible. In addition, most of those experiments strived to avoid thermal gradients in the system. However, even at moderate temperatures the presence of temperature gradients is inevitable due to appreciable liquid evaporation at the gas/liquid interface. A relevant case with particular technological significance is that of a liquid which depressurizes in the presence of dissolved non-condensable gases close to its saturation temperature. Such experiments are complicated to investigate under terrestrial conditions because gravity yields natural convection currents and makes the bubbles to distort from their spherical shape and depart when they are still small. A microgravity environment would circumvent these effects and would further allow considerably large bubbles to be examined where the capacity of optical diagnostics is higher.

Pool boiling experiments in presence of non-condensable gas have been performed in the SOURCE experimental setup which has flown in the sounding rocket Maser 11 attaining microgravity conditions for several minutes. The SOURCE experimental set-up consists of a small cylindrical reservoir of 60 mm diameter and 271 mm long partly filled with a liquid refrigerant HFE7000 pressurized by gaseous nitrogen. The experiment has been described in detail in [5]. At the tank bottom, a heated plate of 1 cm^2 is located to study nucleate boiling regimes in microgravity (see Fig. 2). This plate is equipped with a thermocouple and a flux-meter (uncertainty ±80 W/m^2) to measure the wall heat transfer. Before the launch of the rocket, the reservoir is overheated and pressurized with Nitrogen at a pressure of 3 bar. The sequence of the

* Corresponding author.
E-mail address: karapant@chem.auth.gr (T.D. Karapantsios).

http://dx.doi.org/10.1016/j.ijthermalsci.2016.03.016
1290-0729/

experiment is described in Fig. 1:

- after take-off (time t = 0s) the rocket accelerates during the ascent,
- at t = 50s the microgravity period starts,
- from t = 65s to t = 88s, the tank is filled with the refrigerant HFE7000 at 25 °C,
- from t = 88s to t = 190s, the free surface stabilizes, the refrigerant evaporates in the wall vicinity, then the concentration of the HFE7000 vapour in the gas phase increases close to the tank wall. The non-uniformity of HFE7000 vapour concentration in the gas phase along the interface leads to a strong Marangoni convection.
- At t = 190s, the tank pressure is reduced from P = 3.35 bar–1.82 bar to initiate nucleate boiling.
- From t = 200s to t = 263s, the small plate is heated and nucleate boiling takes plate in subcooled condition. The liquid temperature is smaller than saturation temperature.
- At t = 263s, the tank pressure is reduced from 1.93 bar to 1.23 bar.
- From t = 320s–380s, heat transfer and bubble size evolution in saturated boiling condition is investigated. The results obtained in subcooled and saturated boiling conditions have been reported in [6].

Pictures of the different steps of the experiments are shown in Fig. 2.

In the present paper, we focus on investigating the depressurization phase between t = 263s and 324s, which is a period lying between the sub-cooled and the saturated boiling phases. During this phase, the wall heat flux is kept constant and equal to 1.36 W/cm^2 and the wall temperature T_0 is equal to 51 °C. In this phase of the experiment, a bubble remaining on the heated plate after the end of the subcooled boiling period continues to grow. This is a result of different contributions such as volume expansion due to depressurization, desorption of dissolved non-condensable gas, rise of vapour pressure. The evolution of the radius of the large bubble during the depressurization is measured by image processing. At t = 263s, the bubble radius is equal to R_o = 4.18 mm. While the pressure decreases by a factor of 1.57, the bubble radius increases by a factor of 3.05.

The temperature of the gas inside the bubble is also measured at different locations (Fig. 3). An array of 5 thermocouples is placed above the heated plate. Thermocouple T_{14}, T_{16} and T_{17} are located 1.59, 4.27, 8.69 mm above the heated wall, respectively. The liquid bulk temperature T_L measured above the bubble and the saturation temperature at the tank pressure T_{sat} are also plotted in Fig. 3. Temperature measurements are quite noisy but although absolute values are within thermocouple uncertainty (±0.1 °C) the observed fluctuations (sensitivity) are real and reflect the dynamic nature of the observed phenomena. In particular, thermocouple T_{16} shows a marginal increasing trend in temperature evolution. A temperature rise of 1 °C during the decompression period is recorded by thermocouple T_{17} but the measurement noise prevents to recognize the exact time evolution of this rise. Finally, the thermocouple T_{14} undergoes a temperature increase of 3 °C with most of it occurring sharply at t = 305s which appears to be the moment at which the thermocouple pierces the bubble. The thermocouples T_{14}, T_{16} and T_{17} are located inside the large bubble for a significant part of the depressurization. Then a gradient of temperature inside the gas phase can be evaluated at a value around 2 K/cm. T_{17} measures an average temperature of 33.8 °C, which corresponds to a partial pressure of HFE7000 vapour P_v = 0.96 bar, whereas T_{14} which measures an average temperature of 35.8 °C, corresponding to P_v = 1.03 bar. These temperatures are almost unchanged during the end of the depressurization after t = 300s.

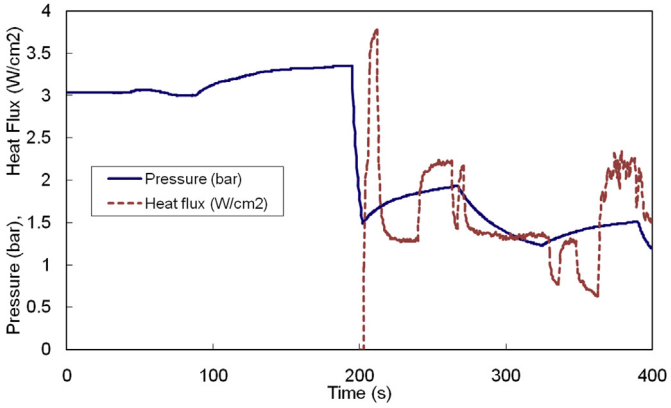

Fig. 1. Sequence of the experiment Source.

A direct modeling approach is extremely difficult since the problem is a combination of degassing and evaporation [7,8]. The plate in contact with the bubble is heated and this creates a temperature distribution in the liquid. As the system pressure decreases it is possible that the temperature of the solid in contact with the bubble gets close or even exceeds the boiling temperature of the liquid. However, the average temperature of the bubble remains colder than the one of its base and this average temperature governs bubble growth. In any case, all the complexities associated with microlayer evaporation may be present. The information given by the measured temperatures in the liquid is limited since the temperature profile in the liquid can be very complex and the connection between the fixed in space thermocouples and the actual average bubble temperature is rather weak.

In addition to the effort needed to deal with the heat transfer problem, the mass transfer equations for the dissolved gas in the liquid domain must be solved. In particular, handling of Marangoni motion for a growing bubble requires a big computational effort [9]. So detailed modeling of the process requires state of the art elaborate computational tools and it is out of the scope of the present work. The alternative approach followed here is to build step by step simplified models incorporating basic aspects of the process and compare to the experimental curve in order to assess the phenomena determining the bubble growth. In this respect, the first step is to develop an isothermal 1-D bubble growth model for which an approximate analytical solution can be derived (i.e. assuming as bubble temperature the time average value of thermocouples measurements). The second step is to extend the analytical solution in order to account for the 2-D nature of the liquid domain (due to existence of the hot plate) and for a steady linear temperature profile in liquid. The above scenarios yield results that can not explain the experimental curve so a time variation of the average bubble temperature is considered, next. A numerical technique for the corresponding non-isothermal 1-D bubble growth problem is developed. Finally, an inverse problem of computing the average bubble temperature evolution corresponding to the experimental growth curve is set up and solved.

2. Formulation of 1-D radial symmetric model for isothermal bubble growth

The mathematical model which describes the depressurization stage of bubble growth in the present experiment refers to the growth of a pre-existing gas bubble inside a volatile liquid during the reduction of the external (with respect to the bubble) pressure

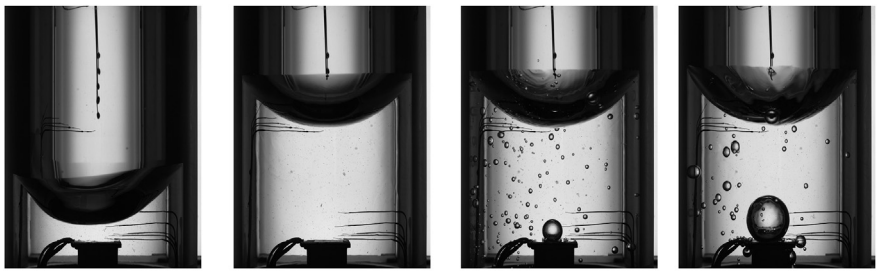

Fig. 2. Pictures of the different sequences of the experiment: (a) tank filling; t = 73 s, (b) Marangoni convection at the free surface; t = 155 s, (c) subcooled boiling; t = 240 s, (d) saturated boiling; t = 370 s.

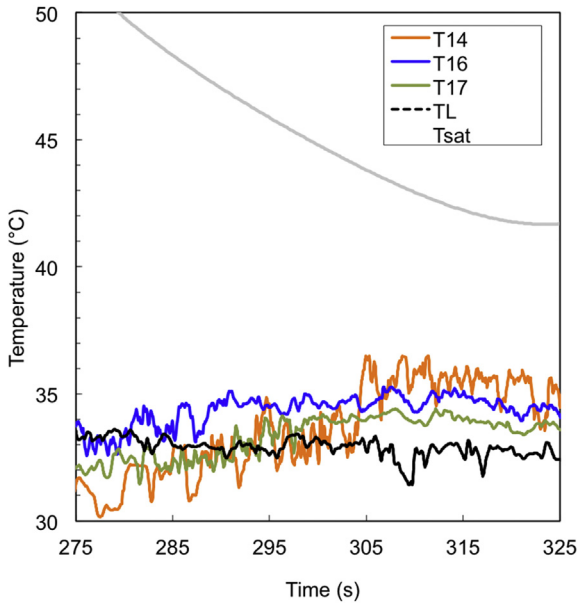

Fig. 3. Thermocouple location and temperature evolution during the depressurization stage.

of the system. The pressure-time function is given as $P_{ex}(t)$ where t denotes time. According to experimental temperature measurements, the temperature in the bubble and in the liquid close to the bubble does not vary radically in space and time so at a first approximation it can be considered constant. The temperature (relative) uniformity (despite the localized heating from the hot plate at the base of the bubble) can be ascribed to Marangoni motion (leading to convection and mixing) imposed by the surface of the bubble. The effect of the existence of the hot plate is ignored at a first approximation assuming a spherical 1-D geometry for bubble growth. The formulation of the mathematical problem for bubble growth in a volatile liquid, i.e. of appreciable vapour pressure, undergoing a pressure variation follows:

If R(t) is the bubble radius and r the radial coordinate, the radial velocity u in the liquid around the bubble results from the continuity equation as $u = \frac{R^2}{r^2}\frac{dR}{dt}$ [10]. Bubble dynamics is described from the well known Rayleigh–Plesset equation [11] which for the time scale of the present problem degenerates to the simple pressure balance:

$$P_g + P_v = P_{ex} + \frac{2\sigma}{R} \tag{1}$$

where P_g is the gas pressure in the bubble, P_v is the pressure of the vapour in the bubble (equal to vapour pressure) and σ is the surface tension of the liquid. Although for newly generated bubbles the surface tension term is always important, it can be easily verified that it is small and it can be safely ignored for pre-existing bubbles with size higher than 100 μm which are of interest in the present work.

The mass conservation equation for the gas dissolved in the liquid includes accumulation, convection and diffusion terms and can be written as [12]:

$$\frac{\partial c}{\partial t} + u\frac{\partial c}{\partial r} = D\left(\frac{\partial^2 c}{\partial r^2} + \frac{2}{r}\frac{\partial c}{\partial r}\right) \tag{2}$$

where c is the molar concentration of the gas in the liquid phase and D is the gas molecular diffusivity in the liquid. The global mass balance of the gas in the bubble (where instantaneous perfect mixing between the gas and the vapour occurs) is [13]:

$$\frac{d\rho_g R^3}{dt} = 3R^2 D\left(\frac{\partial c}{\partial r}\right)_{r=R} \tag{3}$$

where ρ_g is the molar gas density in the bubble. The above equation states that the accumulation of gas in the bubble equals to the amount of gas that enters the bubble by mass transfer from the liquid. In its derivation, the relations for the volume and the surface area of the bubble have been used. The gas density is related to the pressure of the gas through the ideal gas law $\rho_g = P_g/R_gT$ where R_g is the universal gas constant and T is the temperature. The solubility of the gas in the liquid c_{eq} can be found from the following version of the Henry law [14]:

$$c_{eq} = \frac{P_g}{H}\rho_f \tag{4}$$

where the Henry constant H has pressure units such as the ratio P_g/H to be the equilibrium molar fraction of the gas in the liquid, and ρ_f is the liquid molar density. The initial and boundary condition of the problem is that the dissolved gas concentration is the saturation concentration at the initial external pressure P_o=$P_{ex}(t = 0)$ and the initial bubble radius is R_o. It is assumed that the mass transfer rate of gas towards the free surface of the liquid in the experimental container is small and so is incapable of reducing considerably the dissolved gas concentration in the bulk of the liquid. It is noted that the above model considers implicitly interfacial evaporation (through inclusion of vapor pressure contribution). The only assumption is that evaporation is fast compared to gas diffusion which is clearly valid considering the small diffusion coefficient in the liquid and the heat availability in the system.

From the physical point of view, as the external pressure drops

the gas pressure in the bubble also drops and so also does the gas solubility in the liquid according to Equation (4). This means that the liquid phase is oversaturated by dissolved gas which therefore starts to diffuse towards the bubble. In parallel, the gas already existing in the bubble expands in order to follow the external pressure reduction. The gas composition in the bubble changes because P_v does not follow the external pressure variation but it is constant. The instantaneous molar fraction of vapor is $P_v/P_{ex}(t)$.

3. Approximate analytical solution of the 1-D problem of isothermal bubble growth

The above system of equations comprises a closed problem which must be solved for the evolution of R. The problem of instantaneous decompression (step pressure reduction) leads to an autonomous problem for which an analytical solution exists (the so called self-similar solution) for growth from zero initial radius [10,15]. In the present case where the pressure reduction is a function of time a numerical solution is necessary. The problem includes a partial differential equation with a free boundary and its solution is not trivial. The usual approach is the boundary immobilization which leads to the appearance of new highly convective terms in the transformed equation requiring special techniques for their resolution [16,17]. Here a different approach will be followed as a first step to solve approximately the problem based on the existing exact solutions. The key parameter of the mass-transfer dominated bubble growth problem is the so called Foaming number, F [18], which is a measure of the growth velocity of the bubble. For the present problem, F is time dependent through the pressure variation and is given as

$$F = \frac{c_o - c_{eq}(t)}{\rho_g} = \left(\frac{P_o - P_{ex}(t)}{P_{ex}(t) - P_v}\right)\frac{R_g T}{H}\rho_f \tag{5}$$

As long as ρ_g is constant and can go out of the derivative in Equation (3) the bubble growth problem can be solved analytically even for a non constant F number. In the limit $F << 1$ diffusion dominates over convection and the concentration profile is given from the steady state diffusion equation [19]. In the other limit of convection domination, $F >> 1$, a thin concentration boundary layer is developed around the bubble and the problem can be solved by assuming low-order polynomial concentration profiles [20]. The two limiting cases are unified by using a generalized Churchill interpolation scheme [21] with criterion the satisfactory approach to the exact self-similarity solution for constant F [22].

In the present case the situation is more complex since ρ_g varies with time through pressure and it should stay in the derivative in Equation (3). Then, Equation (3) can be written as

$$\rho_g\frac{dR^3}{dt} + R^3\frac{d\rho_g}{dt} = 3R^2 D\left(\frac{\partial c}{\partial r}\right)_{r=R} \Rightarrow \frac{dR^2}{dt} + \frac{2R^2}{3}\frac{d\rho_g}{\rho_g dt} = \frac{2DR}{\rho_g}\left(\frac{\partial c}{\partial r}\right)_{r=R} \tag{6}$$

The right hand side of the final equation which represents the contribution of mass transfer on bubble growth is approximated by the term derived in [22] for the case of constant ρ_g. In addition, ρ_g in the second term is written in terms of pressure using the ideal gas law and the pressure balance. The final equation takes the form:

$$\frac{dR^2}{dt} + \frac{2}{3}R^2\frac{d\ln(P_{ex} - P_v)}{dt} = \left[(2DF)^{0.8} + \left(\frac{12}{\pi}DF^2\right)^{0.8}\right]^{1.25} \tag{7}$$

where arbitrary pressure units can be used in the logarithm without altering the results. The first term in the brackets in the right stands for the diffusion dominated regime and the second term for the convection dominated regime, respectively. The above differential equation is linear with respect to R^2 so it can be solved analytically to give the final result:

$$R = \left[R_0^2\left(\frac{P_o - P_v}{P_{ex} - P_v}\right)^{2/3} + \frac{1}{(P_{ex} - P)_v^{2/3}}\int_0^t \left[(2DF)^{0.8} + \left(\frac{12}{\pi}DF^2\right)^{0.8}\right]^{1.25}(P_{ex} - P_v)^{2/3}d\tau\right]^{1/2} \tag{8}$$

This equation is an approximate analytical solution to a complicated mathematical problem requiring specialized numerical techniques, and it is constructed by patching known asymptotic solutions. Let us examine this equation in detail. In the absence of mass transfer the equation reduces to the exact result that the bubble radius is inversely proportional to the gas partial pressure at the 1/3 power. In the case of constant pressure it reduces to the mass transfer problem solution proposed in [22] for the entire F range. An additional case in which the above solution is exact is the case of $F<<1$ (including pressure variation). This happens because the gas expansion due to pressure profile does not interfere with the mass transfer process being always in pseudo-steady state. On the contrary, an error is expected in case of $F>>1$ (convection domination) because the corresponding term has been derived accounting only the mass transfer growth velocity.

Having developed the mathematical model of the process let's examine now what is the expected behaviour of a bubble during the particular experiment considered here. The uniform temperature of the bubble is assumed to be 34.5 °C based on the measured temperatures in the bubble. The physical parameters of the system N_2-HFE7000 at this temperature are employed. The experimental system pressure P_{ex} and the Foaming number F are shown versus time in Fig. 4. The driving force for mass transfer is small at the beginning because the bulk concentration of gas in the liquid is equal to the equilibrium one. As the pressure is reduced the situation changes and F increases up to 1.5. It is noted that in the present problem F is in the transition region between diffusion and convection so the complete theory for the transition region is necessary.

The evolution of the ratio of the instantaneous bubble radius to the initial bubble radius for several values of the initial radius is shown in Fig. 5. As the bubble radius increases its specific surface (surface per unit volume) decreases so the contribution of mass transfer to bubble growth decreases. The growth curve for the case of no mass transfer (pure gas expansion) being independent from R_o is also shown. At short time the small driving force leads to a small mass transfer contribution to growth for all initial bubble sizes. As time elapses the driving force for growth increases and the mass transfer contribution increases with time and decreases with the initial bubble radius, being practically zero for $R_o > 3$ mm. This

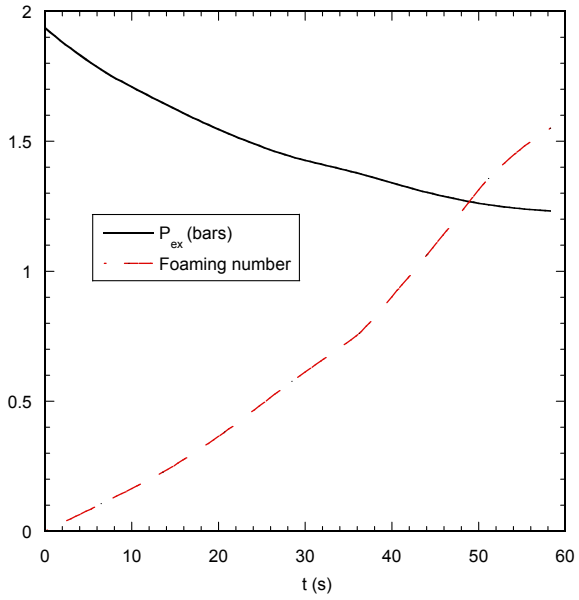

Fig. 4. Bulk pressure P_{ex} and Foaming number F evolution during the experiment.

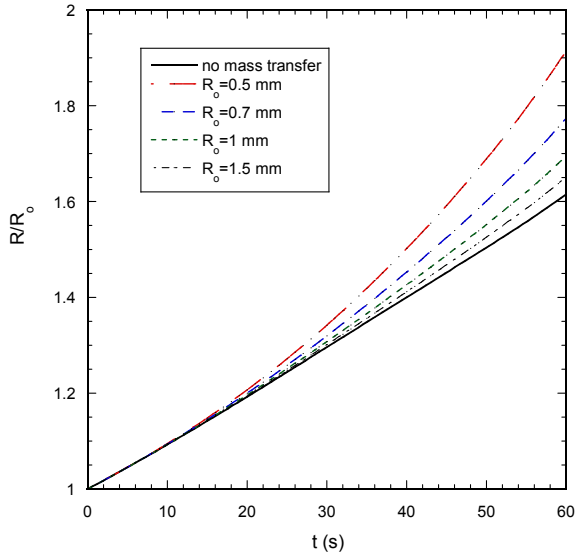

Fig. 5. Evolution of the computed ratio R/R_o of instantaneous to initial bubble radius during the experiment for several values of the initial bubble radius R_o.

behavior is better depicted in Fig. 6 where the radius R/R_o is displayed versus the initial radius at two values of time. The no mass transfer asymptotes are also shown (horizontal lines). It is clear how the mass transfer contribution to growth decreases to zero as the initial bubble radius increases. It is noted that the experimental value for the ratio R/R_o at $t = 60$ s is at about 3.05 (see Fig. 10 for the complete experimental bubble growth curve) whereas the theoretical value is at about 1.6. Although this result is based on an approximate solution, the deviation of the resulting growth curve from the experimental one (corresponding to $R/R_o = 3.05$) renders clear that the above model is not capable of explaining the experimental behavior.

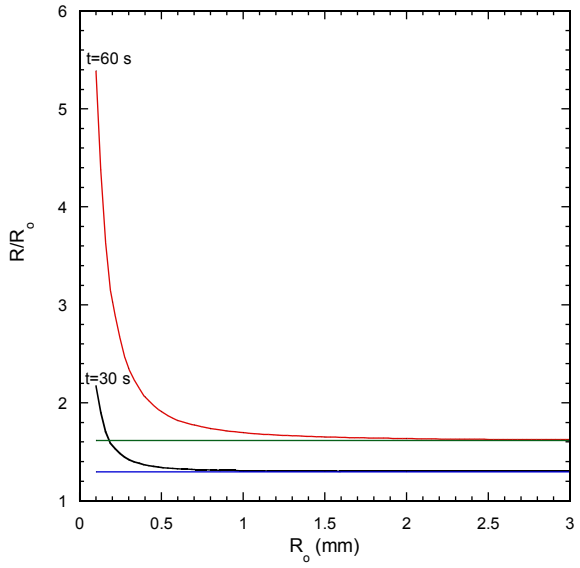

Fig. 6. Computed ratio R/R_o between bubble radii at time t (30 s and 60 s) versus initial bubble radius R_o.

4. Extension of analytical solution to account for 2-D effects and for a temperature profile in the liquid

In this section the analytical solution is extended to account for 2-dimensionality and for the presence of a temperature profile in the liquid seeking to explain the deviation between theoretical and experimental growth curve. In order to estimate the effect of the small temperature decrease measured experimentally in the bubble during its growth, a linear temperature profile in the liquid is assumed. This profile is time-independent suggesting that the bubble is exposed to colder fluid as it grows. In addition to the effect of the non-uniform temperature the influence of the 2-dimensionality of the actual geometry (i.e. growth on a hot plate and not in an infinite medium) is explored. The following temperature profile in the liquid is assumed: $T = T_o - \alpha x$ where x is the distance from the plate and T_o is the temperature of the bubble base (see Fig. 7). It is stressed that the latter has not to be equal to the measured plate temperature since such a measurement refers to intra-solid temperature which is different from the solid–liquid interfacial temperature T_o. The gas diffusivity in the liquid and the Henry coefficient exhibit a temperature dependence leading to a distribution of degassing rate at the surface of the bubble. The complete mathematical problem is exceedingly difficult to solve. The transient diffusion convection equation must be solved in the domain with a moving boundary in 2-D. Here, the procedure followed in the case of 1-D problem i.e. patching of existing

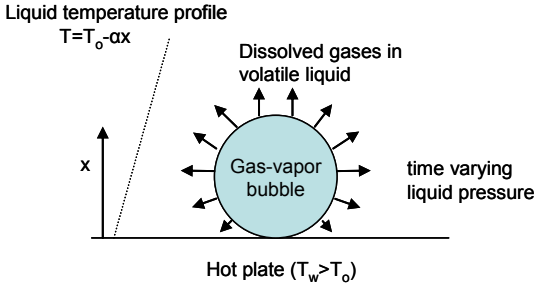

Fig. 7. A schematic of the bubble growing in a steady linear temperature profile.

asymptotic solutions is extended to the 2-D case. The direct effect of Marangoni motion (which is considered implicitly through the assumed temperature profile) on the mass transfer procedure is ignored (radial motion is considered more important than tangential). In the 2-D case the gas density and gas composition are non-uniform in the bubble and this is taken into account in the derivation of the growth equations. The temperature and vapour molar fraction distributions in the bubble are given by the solution of the Laplace equation with the following boundary condition on the bubble surface:

$x_v = P_v(T_o - \alpha x)/P_{ex}$ for vapour molar fraction (9)

$T_g = T_o - \alpha x$ for gas temperature (10)

The Laplace equation in spherical geometry with the above boundary conditions must be solved to find the intra-bubble temperature and vapour molar fraction distributions. Then the average gas density can be computed from the following integral over the bubble volume (V_b is the bubble volume).

$$\rho_{gave} = \frac{1}{V_b}\int_{V_b}(1-x_v)\frac{P_{ex}}{R_g T_g}dV \tag{11}$$

The above procedure is very cumbersome including the solution of two elliptic partial differential equations and the computation of an integral in two dimensions. An alternative much simpler approximate procedure is followed. Taking into account the fact that the spatial density variation in the bubble is expected to be small due to small temperature variation, the following approximation can be used:

$$\rho_{gave} = \frac{1}{V_b}\int_{V_b}(1-x_v)\frac{P_{ex}}{R_g T_g}dV \approx (1-x_{vave})\frac{P_{ex}}{R_g T_{gave}} \tag{12}$$

$$T_{gave} = T_o - \alpha R \tag{13}$$

$$x_{vave} = \frac{1}{2P_{ex}}\int_{-1}^{1} P_v(T_o - \alpha R(1-z))dz \tag{14}$$

Substituting Equations (13) And (14) in (12) the following relation for the average gas density results in:

$$\rho_{gave} = \left[1 - \frac{1}{2P_{ex}}\int_{-1}^{1} P_v(T_o - \alpha R(1-z))dz\right]\frac{P_{ex}}{R_g(T_o - \alpha R)} \tag{15}$$

The next assumption is that during the growth of the bubble, mass transfer at each position of the surface occurs at the same rate with that of a bubble undergoing axisymmetric growth at the local conditions. These conditions include the gas solubility and diffusivity (through their temperature dependence) and the local growth velocity. The geometry of the growth (sphere attached to the wall) leads to a distribution of the growth velocity with the azimuthal angle from zero at the wall side to 2 dR/dt at the liquid side. The correction with respect to local growth velocity is taken into account by multiplying with a correction coefficient the high foaming number component of the bubble growth term for axisymmetric growth derived in the previous section. Another correction is needed for the pure diffusion component of the growth rate. This correction is needed to take into account the influence of the wall presence on the solution of the corresponding diffusion equation. From the solution of the corresponding Laplace equation for the plane-sphere geometry a correction factor $\delta = 0.693$ was found [24]. Following the same procedure used for the derivation of the growth equation in the 1-D case and taking an integral over the bubble surface for the mass transfer term leads to the following equation

$$\frac{dR^2}{dt} + \frac{2}{3}R^2\frac{d\ln\left(\rho_{gave}\right)}{dt} = \int_{-1}^{1} D(T_o - \alpha(1+z)R)\left[(2\delta F)^{0.8} + \left(\frac{12}{\pi}(1+z)F^2\right)^{0.8}\right]^{1.25}dz \tag{16}$$

where x_{vave} and T_{gave} are the average bubble vapour fraction and temperature respectively.

Furthermore it can be shown that for harmonic functions (i.e. functions obeying the Laplace equation) volume averages are equal to surface averages (see [23]). Thus x_{vave} and T_{ave} can be found by simply integrating the corresponding quantities (Equations (9),(10)) over the surface of the bubble avoiding the solution of the Laplace equation. These integrations after some algebra and transformation of integration variables (z=(x-R)/R) result in:

The Foaming number is also position dependent in this case and it can be computed as

$$F = \frac{c_{eq}(t) - c_o}{\rho_g} = \left(\frac{P_{ex}(t)(1-x_{vaveo})}{\rho_g}\right)\frac{\rho_f}{H(T_o - \alpha(1+z)R)} \tag{17}$$

It is noted that the units of ρ_g in Equation (16) do not influence the results and x_{vaveo} is the initial average vapour molar fraction in the bubble. The Equation (17) can be integrated in closed form to give:

$$R = \left[R_o^2\left(\frac{(1-x_{vaveo})T_{gave}}{(1-x_{vave})T_{gaveo}}\right)^{2/3} + \left(\frac{1-x_{vaveo}}{T_{gaveo}}\right)^{2/3}\int_0^t\int_{-1}^{1} D(T_o - \alpha(1+z)R)\left[(2\delta F)^{-0.8} + \left(\frac{12}{\pi}(1+z)F^2\right)^{-0.8}\right]^{-1.25}dz\left(\frac{T_{gave}}{1-x_{vave}}\right)^{2/3}d\tau\right]^{1/2} \tag{18}$$

where T_{gaveo} is the initial average bubble temperature equal to $T_o - \alpha R_o$. The evolution of the bubble radius can be easily computed numerically by using the trapezoidal rule for both the integration levels in Equation (18). The trapezoidal rule is also used for the computation of average gas density at each time step from Equation (15). As it has been already shown, for the present experimental conditions the effect of mass transfer on bubble growth is negligible for $R_o > 2$ mm (gas expansion limit). Let's examine now, how a non-uniform bubble temperature may influence bubble growth in this limit. Ignoring mass transfer, the bubble radius evolution equation takes the form:

$$R = R_o\left(\frac{(1-x_{vaveo})T_{gave}}{(1-x_{vave})T_{gaveo}}\right)^{1/3} = R_o\left[\frac{P_o - 0.5\int_{-1}^{1} P_v(T_o-\alpha R_o(1-z))dz}{P_{ex} - 0.5\int_{-1}^{1} P_v(T_o-\alpha R(1-z))dz}\,\frac{T_o-\alpha R}{T_o-\alpha R_o}\right]^{1/3} \quad (19)$$

An extensive mathematical procedure including Taylor expansion around T_o for the vapor pressure relation, integration of the resulting integrals and a linear expansion of the resulting relation with respect to the growth relation at constant temperature T_o results in:

$$\frac{R}{R_o} = \left(\frac{R}{R_o}\right)_{T=T_o}\left[1 - C_f\right] \quad (20)$$

where the correction factor accounting for the temperature non-uniformity is given as:

$$C_f = \alpha P'_v(T_o)\left(\frac{R}{P_{ex}-P_v(T_o)} - \frac{R_o}{P_o - P_v(T_o)}\right) + \frac{\alpha}{T_o}(R - R_o) \quad (21)$$

The prime denotes differentiation of the function with respect to its argument (i.e. $P'_v(T) = \frac{dP_v}{dT}$). The reduction of growth rate with the reduction of bubble temperature as the bubble grows has two contributions: reduction of vapor pressure which means more space for the gas and smaller growth rate (first term in Equation (21)) and increase of gas density (second term in Equation (21)). The first contribution is the dominant one. A representative value of temperature non-uniformity (temperature gradient) in the present experimental conditions is at about 2 K/cm so this order of magnitude for α is considered here. The correction factor for $\alpha = 1$ K/cm and several values of R_o for the described experiment is shown in Fig. 8. Unlike the growth rate for uniform temperature the correction factor now depends on the initial radius R_o. According to Equation (21), C_f is proportional to α so the correction factor for other values of α can be found by a simple multiplication of the values shown in Fig. 9. The correction is in any case less than 2%. This means that it can be made considerable for α larger than 3 K/cm. Nevertheless it must be kept in mind that the above analysis was made having the wall temperature as reference which is a worst case scenario. If another temperature such as the initial average bubble temperature or a representative mean bubble temperature during the bubble growth is chosen for reference (as it was done in the 1-D model where a representative experimental temperature was considered) the correction factor would be one order of magnitude smaller.

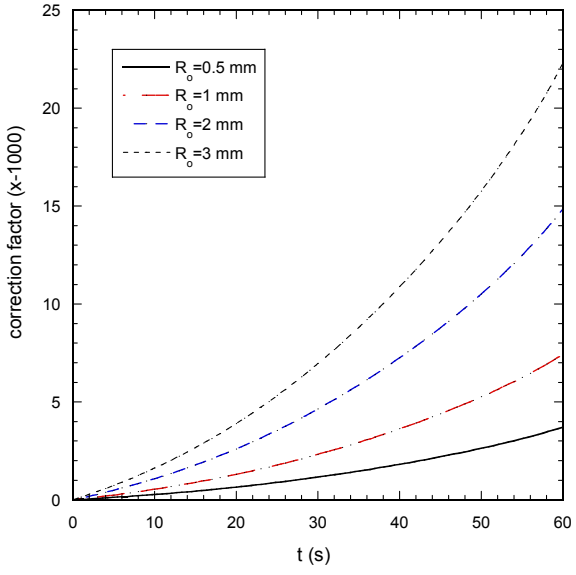

Fig. 8. Correction factor C_f ($\times$ 1000) for bubble growth in temperature field with slope 1 K/m in the absence of mass transfer.

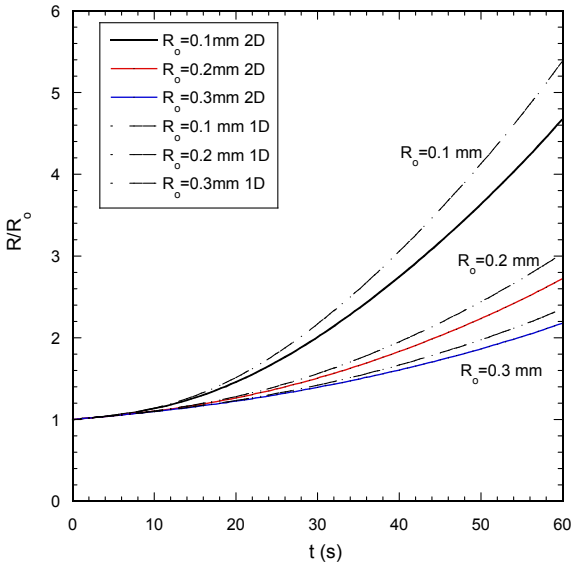

Fig. 9. Evolution of the ratio R/R_o for small bubbles computed from 1-dimensional and 2-dimensional theories for several values of R_o.

For the general case in which mass transfer is important, the complete theory (Equation (18)) must be employed. It is noticed that small bubbles, for which mass transfer is important, undergo a very small temperature reduction due to their small size. On the other hand, for larger bubbles where a considerable temperature decrease can be met, the contribution of mass transfer to the growth rate is negligible. The evolution of the ratio R/R_o for bubbles with small initial size is shown in Fig. 9. In the plot, the corresponding curves computed for the 1-D model are also shown. The existence of the temperature distribution has no influence at these results even for values of α much larger than those considered representative of the experiment examined here. The 2-D model shows appreciably slower bubble growth due, mainly, to the factor δ used for the conduction term and, secondary, to the radial velocity distribution for the convection term. So, although the temperature distribution in the bubble can be safely ignored, the 2-D model is more correct (slower growth) for a bubble growing on the wall than the 1-D model which corresponds to a bubble growing in the bulk liquid (faster growth).

Summarizing, a semi-analytical relation was derived for the growth of pre-existing bubbles in the bulk liquid or on a solid wall during transient behaviour of the bulk pressure. It was shown that temperature gradients in the liquid of the order of a few K/cm have negligible effect on the bubble growth behavior. Nevertheless, the corrections due to 2-dimensionality and to temperature profile in the liquid are not capable to explain the deviations between theoretical and experimental growth curves.

5. Numerical solution for the 1-D problem with evolving bubble temperature

So far our modeling efforts were based on the assumption of constant in time temperature profile. According to the above approximate model the ratio of the final to initial bubble radius is equal to the ratio of the initial to final gas pressure in the bubble raised to the 1/3 power. This leads to a final bubble size much smaller than the experimental one. This might be attributed to the experimental fact that the actual temperature profile in the liquid is not constant but evolves gradually with time. Yet, direct modeling of this evolution is extremely complex as it has been discussed in the introductory section. The key effect of a liquid temperature profile on bubble growth is the increase of vapor fraction inside the bubble. As it has been shown in the previous section, the vapor fraction depends on the average bubble temperature (equal to the average gas–liquid interface temperature). As this temperature is not known (and actually it is not experimentally accessible) an inverse problem approach will be followed: what is the average bubble temperature evolution (or equivalent vapor pressure evolution) that leads to the measured growth curve? The mathematical problem is still described by Equations (1)–(4) but a numerical solution technique has to be implemented now. The governing equations are of the transient convection-diffusion type in a semi-infinite domain with a moving boundary and their numerical solution is not trivial. A standard procedure is the immobilization of the moving boundary by using a new spatial variable $y^3 = r^3 - R^3$ (Lagrangian transformation). This choice has the advantage of eliminating the convection terms [16,17]. On the other hand, the required concentration profiles are extremely steep with respect to the new variable. This makes necessary a new (fixed in time) transformation of variable which has as a consequence the reappearance of the convection terms. So, the advantage of the above variable transformation vanishes. The alternative Lagrangian transformation $y = r/R$ is more meaningful from a physical point of view.

By using the following chain differentiation rule

$$\frac{\partial X(r,t)}{\partial t} = \frac{\partial X(y,t)}{\partial t} + \frac{\partial X}{\partial y}\frac{\partial y}{\partial t} \tag{22}$$

the system of equations is transformed to

$$\frac{\partial c}{\partial t} = \frac{1}{y^2R^2}\frac{\partial}{\partial y}y^2\frac{\partial c}{\partial y} + \frac{dR}{dt}\frac{1}{R}\left(y - \frac{1}{y^2}\right)\frac{\partial c}{\partial y} \tag{23}$$

$$\frac{dR}{dt} = -\frac{R}{3}\frac{d\ln(P_{ex}(t) - P_v(t))}{dt} + A\frac{P_{ex}(0) - P_v(0)}{P_{ex}(t) - P_v(t)}\frac{1}{R}\left(\frac{\partial c}{\partial y}\right)_{y=1} \tag{24}$$

with initial condition $c(y,0) = 1$ and boundary conditions $c(\infty,t) = 1$ and $c(1,t) = (P_{ex}(t) - P_v(t))/(P_{ex}(0) - P_v(0))$. The variables in the above system are normalized as follows: R by its initial value R_o, c by its initial value c_o and t by the diffusion characteristic time R_o^2/D. The parameter A is given as $R_gT\rho_f/H$. Even after immobilization any attempt to directly discretize the semi-infinite liquid domain leads to numerical problem. This is due to the steep concentration profiles (boundary layers) appearing at the first stages of the growth. The problem is overcome by a clustering of the discretization points close to the bubble. This can be achieved by introducing the new independent variable z related to y via the relations:

$$z = 1 - e^{-\beta(y-1)} \qquad y = 1 + \frac{1}{\beta}\ln\left(\frac{1}{1-z}\right) \tag{25}$$

Substitution in Equations (23, 24) and performing the algebra leads to the following system:

$$\frac{\partial c}{\partial t} = \frac{1}{y^2R^2}\beta^2(1-z)\frac{\partial}{\partial z}(1-z)y^2\frac{\partial c}{\partial z} + \frac{dR}{dt}\frac{1}{R}\left(y - \frac{1}{y^2}\right)\beta(1-z)\frac{\partial c}{\partial z} \tag{26}$$

$$\frac{dR}{dt} = -\frac{R}{3}\frac{d\ln(P_{ex}(t) - P_v(t))}{dt} + A\frac{P_{ex}(0) - P_v(0)}{P_{ex}(t) - P_v(t)}\frac{\beta}{R}\left(\frac{\partial c}{\partial z}\right)_{z=0} \tag{27}$$

The boundary conditions take the form $c(1,t) = 1$ and $c(0,t) = (P_{ex}(t) - P_v(t))/(P_{ex}(0) - P_v(0))$.

The above equations are discretized using a second order finite difference scheme. The resulting system of ordinary differential equations is integrated using an implicit Runge-Kutta solver [25]. A typical value for β is $\beta = 1$. Larger values are needed for very steep concentration profiles. A trial and error procedure is needed to select an appropriate value of β having as criterion the smoothness of the resulting solution.

Results of growth curves for several choices of the vapor pressure evolution curve are shown in Fig. 10. Curve 4 corresponds to constant $P_v = 1$ bar which is very close to those used in previous calculations. The contribution of mass transfer to bubble growth is small compared to the contribution of pressure variation. The corresponding growth curve for $P_v = 1.1$ bar is curve 5. At large times the external pressure approaches too close to vapor pressure and this explains the explosive growth. The shape of the two curves for $P_v = 1$ and 1.1 bars shows that the approach of modeling curves to the experimental growth curve 1 is not possible using a constant vapor pressure. A possible scenario to describe the experimental

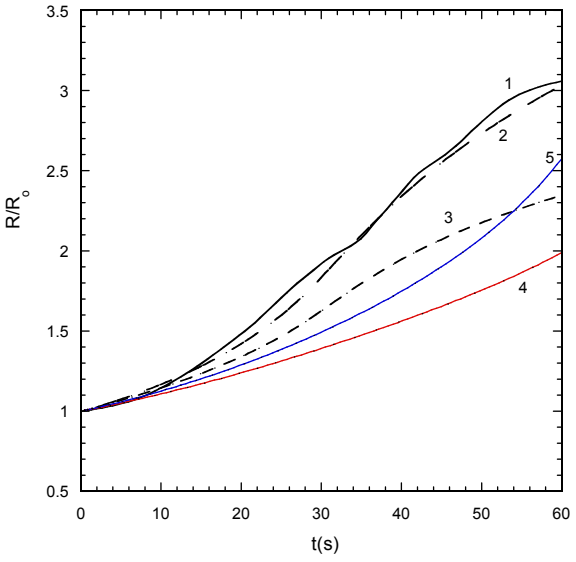

Fig. 10. Bubble radius evolution curves: (1) Experimental (2) Variable vapor pressure (3) Variable vapour pressure with no mass transfer contribution (4) Vapor pressure 1 bar (5) Vapour pressure 1.1 bar.

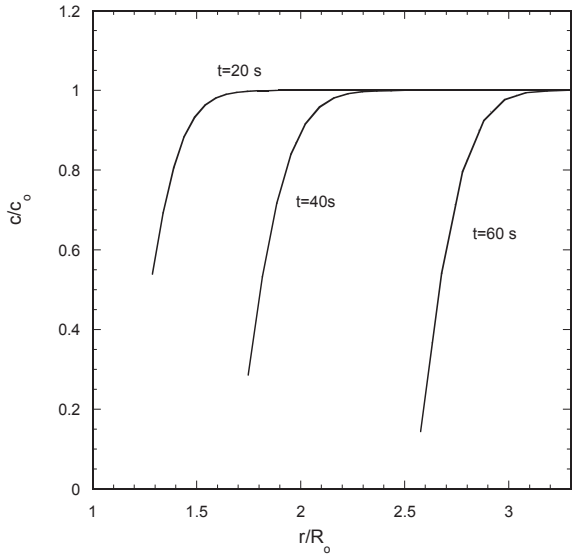

Fig. 11. Evolving gas concentration profiles in the liquid for constant vapour pressure 1.1 bar.

curve is starting with a high initial P_v in order to achieve the initial high growth ratio, followed by its gradual decrease in order to avoid the explosive growth as external pressure decreases. An acceptable approximation of the experimental growth curve is achieved (see curves 1 and 2) by assuming $P_v = 1.25$ bar for the first 30 s and then a linear in time reduction from 1.25 to 0.95 during the next 30 s. This profile was found by a trial and error procedure. An inverse transport phenomena problem can be set up in order to search for the optimum interfacial temperature, i.e., P_v, profile but it is a major task [26] and it is outside of the scope of the present work. Finally, curve 3 shows the growth curve for the chosen profile of P_v in curve 2 but ignoring mass transfer. It is clear that according to the present scenario mass transfer contribution to bubble growth is important. It is noted that the value 1.25 bar found for vapor pressure corresponds to a temperature somewhat larger of 40 °C which is larger than the measured temperatures but it is still much less than the

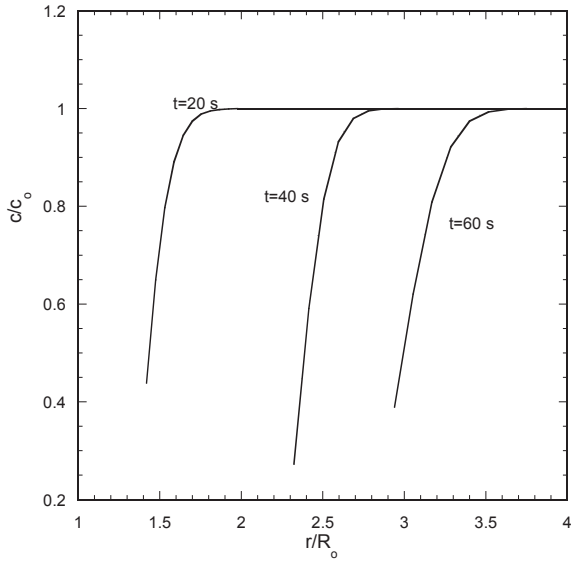

Fig. 12. Evolving gas concentration profiles in the liquid for vapour pressure evolution compatible to the experimental growth curve.

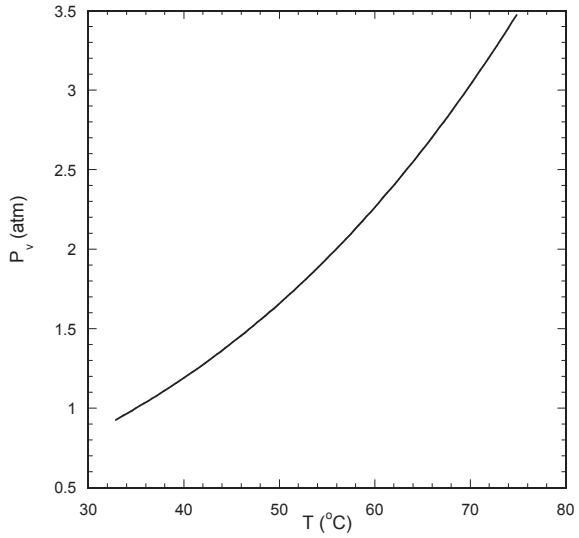

Fig. 13. Relation between vapor pressure P_v and temperature T for HFE7000.

hot plate temperature rendering the assumed average bubble evolution scenario a plausible one.

The dissolved nitrogen dimensionless concentration profiles outside the bubble at three time values for the cases of $P_v = 1.1$ bar and of variable P_v are shown in Figs. 11 and 12, respectively. These profiles have been computed by solving numerically the Equations (26) and (27) considering several temporal profiles of vapor pressure. The left-most lower c/c_o values in each curve correspond to the bubble/liquid interface and $c/c_o = 1$ corresponds to the far bulk locations which are unaffected by the growing bubble. The steepness and different location of the profiles confirm the necessity of the specialized numerical solution techniques such the one developed here. The nitrogen concentration at the bubble/liquid interface decreases with time for constant P_v as it is shown in Fig. 11 and would lead to an explosive growth at large times. The corresponding interfacial concentrations in case of variable P_v (Fig. 12) initially decreases (from t = 20 s to t = 40 s) and then increases (from t = 40 s to t = 60 s) leading to a growth curve similar to the experimental one. Considering $P_v(t)$ (which corresponds to $T_{ave}(t)$) as an undetermined function is the only way to explain the experimentally observed growth curve.

6. Conclusions

A systematic step by step attempt to explain the experimentally observed bubble growth on a heated plate during decompression in the absence of gravity is presented here. Several approximate analytical solutions for 1-D and 2-D bubble growth problems and a specialized numerical technique for the 1-D problem have been developed. The assumption of steady temperature profile (uniform temperature or a linear temperature profile similar to the experimental one) renders the explanation of the experimental growth profile impossible. An inverse bubble growth problem is set-up: Finding the temperature evolution (equivalent to vapor pressure evolution) compatible to the experimental growth curve. It is shown that adopting such an evolution and handling it as fitting variable constitutes the only way to reconstruct and understand the experimental bubble growth curve.

Acknowledgments

The authors would like to acknowledge the European Space

Agency (4200020289-CCN1(AO-2004-111)) and the Centre National d'Etudes Spatiales (RT-NT-22R2200-0501-IMFT) (French space agency) for the flight opportunity of the SOURCE experiment on Maser 11 and for the financial support in this project. The work was performed under the umbrella of COST Actions MP1106 and MP1305.

Appendix A. Vapour pressure-Temperature relation for HFE7000

The vapor pressure P_v of HFE7000 is given (in atm) as function of temperature T (in ^oC) as

$$P_v = 7.4 \cdot 10^{-4} T^2 - 0.0197T + 0.79$$

The above equation can be used to give boiling temperature T_{sat} as function of external pressure P_{ex} by replacing T with T_{sat} and P_v with P_{ex}. The relation between P_v (P_{ex}) and T (T_{sat}) is shown graphically in Fig. 13.

Nomenclature

c	dissolved gas molar concentration
c_{eq}	gas solubility in the liquid
c_o	initial dissolved gas molar concentration
D	diffusion coefficient of gas in the liquid
F	Foaming number
H	Henry constant
P_{ex}	external pressure
P_g	gas partial pressure
P_o	initial external pressure
P_v	vapour pressure
R	bubble radius
r	radial coordinate
R_g	universal gas constant
R_o	initial bubble radius
t	time
T	temperature
u	fluid velocity
V_b	bubble volume
x_v	vapour molar fraction in the bubble
z	axial coordinate (distance from wall)

Greek characters

α	slope of linear temperature profile in the liquid
δ	(=0.693) factor for accounting of 2-Dimensionality in conduction limit
ρ_f	liquid molar density
ρ_g	gas molar density in the bubble
σ	surface tension

References

[1] Payvar P. Mass transfer controlled bubble growth during rapid decompression of a fluid. Int J Heat Mass Transf 1987;30:699–706.
[2] Barker GS, Jefferson B, Judd SJ. The control of bubble size in carbonated beverages. Chem Eng Sci 2002;57:565–73.
[3] Malley JP, Edzwald JK. Concepts for dissolved-air flotation treatment of drinking waters. Water SRT Aqua 1991;40:7–17.
[4] Jones F, Evans GM, Galvin KP. The cycle of bubble production from a gas cavity in a supersaturated solution. Adv Colloid Interface Sci 1999;80:51–84.
[5] Fuhrmann E, Dreyer M. Description of the sounding rocket experiment SOURCE. Microgravity Sci Technol 2009;20:205–12.
[6] Kannengieser O, Colin C, Bergez W. Pool boiling with non condensable gas in microgravity: results of a sounding rocket experiment. Microgravity Sci Technol 2010;22:447–54.
[7] Faghri A, Zhang Y. Transport phenomena in multiphase systems. New York: Academic Press; 2006.
[8] Esmaeeli A, Tryggvason G. Computation of explosive boiling in microgravity. J Sci Comput 2003;19:163–82.
[9] Subramanian RS, Balasubramaniam R. The motion of bubbles and drops in reduced gravity. New York: Cambridge University Press; 2001.
[10] Scriven LE. On the dynamics of phase growth. Chem Eng Sci 1959;10:1–13.
[11] Plesset MS, Prosperetti A. Bubble dynamics and cevitation. Annu Rev Fluid Mech 1977;9:1945–85.
[12] Divinis N, Karapantsios TD, Kostoglou M, Panoutsos CS, Bontozoglou V, Michels AC, et al. Bubbles growing in supersaturated solutions at reduced gravity. AIChE J 2004;50:2369–82.
[13] Patel RD. Bubble growth in a viscous Newtonian liquid. Chem Eng Sci 1980;35:2352–5.
[14] Fogg PGT, Gerrard W. Solubility of gases in liquids: a critical evaluation of gas liquid systems in theory and practice. New York: Wiley Interscience; 1991.
[15] Cable M, Frade JR. Diffusion-controlled growth of multi-component gas bubbles. J Mater Sci 1987a;22:919–24.
[16] Arefmanesh A, Advani SG, Michaelides EE. An accurate numerical solution for mass diffusion induced bubble growth in viscous liquids containing limited dissolved gas. Int J Heat Mass Transf 1992;35:1711–22.
[17] Prousevitch AA, Sahagian DC, Anderson AJ. Dynamics of diffusive bubble growth in magmas. J Geophys Res 1983;98:22283–307.
[18] Lastochkin D, Favelukis M. Bubble growth in variable diffusion coefficient liquid. Chem. Eng J 1998;69:21.
[19] Vrentas JS, Vrentas CM, Ling HC. Equations for predicting growth or dissolution rates of spherical particles. Chem Eng Sci 1983;38:1927–34.
[20] Rosner DE, Epstein M. Effects of interface kinetics, capillarity and solute diffusion on bubble growth rates in highly supersaturated liquids. Chem Eng Sci 1972;27:69–88.
[21] Churchill SW, Usagi R. A general expression for the correlation of rates of transfer and other phenomena. AIChE J 1972;18:1121.
[22] Divinis N, Karapantsios T, de Briyin R, Kostoglou M, Bontozoglou V, Legros J. Bubble dynamics during degassing of dissolved gas saturated solutions at microgravity conditions. AIChE J 2006;52:3029–40.
[23] Kostoglou M, Karapantsios TD. Approximate solution for a nonisothermal gas bubble growth over a spherical heating element. Ind Eng Chem Res 2005;44:8127–35.
[24] Buehl WM, Westwater JW. Bubble growth by dissolution: influence of contact angle. AIChE J 1966;12:571–6.
[25] Villadsen J, Michelsen ML. Solution of differential equation models by polynomial approximation. New York: Prentice Hall; 1978.
[26] Ozisik MN, Orlande HRB. inverse heat transfer, fundamentals and applications. New York: Taylor and Francis; 2000.